Materials Horizons

COMMUNICATION

View Article Online
View Journal | View Issue

Cite this: *Mater. Horiz.*, 2016, 3, 220

Received 26th January 2016,
Accepted 24th February 2016

DOI: 10.1039/c6mh00025h

www.rsc.li/materials-horizons

A stable tetraphenylethene derivative: aggregation-induced emission, different crystalline polymorphs, and totally different mechanoluminescence properties†

Can Wang,[a] Bingjia Xu,[b] Mengshu Li,[a] Zhenguo Chi,[b] Yujun Xie,[a] Qianqian Li[a] and Zhen Li*[a]

Two crystalline polymorphs of TMPE, with the space groups $P2_1(c)$ and $C2$, are cultured from different solvent mixtures and display apparent blue fluorescence with the characteristic of aggregation induced emission (AIE). Excitedly, the $P2_1(c)$ crystal exhibits easily observed mechanoluminescence (ML), while there is no mechanoluminescence for the $C2$ crystal. Careful investigation of their crystal structures and three analogues demonstrates that the special molecule packing of TMPE in the $P2_1(c)$ crystal accounts for its exciting efficient ML performance, providing some information to understand the structure–property relationship of efficient organic ML materials.

Conceptual insights

Organic materials exhibiting mechanoluminescence (ML) are promising for applications in displays, new light sources and pressure sensors *etc.* However, the mechanism for ML generation and the structure–mechanoluminescence relationship remain unclear. Partially due to the aggregation-caused quenching (ACQ) effect caused by π–π stacking interactions, the number of reported organic ML compounds is limited, and their efficiency is generally low. Herein, we present two crystalline polymorphs of a same nonpolar tetraphenylethene derivative TMPE (*i.e.*, the C_p-form and C_c-form) with distinctly different ML activities. Both of the two crystalline polymorphs exhibit brilliant blue PL by the utilization of aggregation-induced emission (AIE) effect and display good stability in air. The block-like C_p-form crystal demonstrates wonderful ML properties, and the highly bright sky-blue emission could be observed under daylight at room temperature. Careful investigation of their crystal structures and three analogues demonstrates that the abundant and intense intermolecular interactions (*i.e.*, C–H···π and C–H···O hydrogen bonds), attributed to the special molecule packing of TMPE in the C_p-form crystal, account for the exciting efficient ML performance. These results provide some information to understand the structure–property relationship of organic ML materials, which will give some guidance for the design of efficient organic ML materials.

Mainly due to strong π–π stacking interactions, normal luminogens suffer badly from aggregation-caused quenching (ACQ) effect, which directly limits their wide application in an aggregated state.[1] In addition to the interest in tackling this problem through different approaches, nowadays, great attention has been devoted to the development of efficient luminogens with the characteristic of aggregation-induced emission (AIE) in the opto-electric field: they are highly emissive in the solid state while showing faint fluorescence when dissolved in a good solvent, as pioneered by the group of Ben Zhong Tang.[2] The inherent mechanism for this AIE phenomenon is ascribed to the restriction of intramolecular motion (RIM) in the aggregates, which could open a radiative pathway for the propeller shaped AIE luminogens, as confirmed by the internal restricted motion of the phenyl ring in the silole, and their external behavior at different temperatures, in solvents with different viscosity, and at different pressures.[3] Among the AIE luminogens developed so far, tetraphenylethene (TPE) is the star molecule, which has been utilized to construct many good AIE gens as promising candidates for applications in LEDs, sensors, *etc.*[4]

Mechanoluminescence (ML) or triboluminescence (TL) is the emission of light caused by the application of mechanical stress to a solid, commonly a crystal or microcrystal phase, and has promising practical application in displays, new light sources and pressure sensors *etc.*[5] Regardless of its long history with the first report in 1605 by Francis Bacon[6] - partially due to the ACQ effect caused by π–π stacking interactions - the lack of efficient ML materials, especially those with emission in the visible region (most reported organic ML compounds emit exclusively in the UV region), hindered the exploration of the mechanoluminescence–structure relationship and further development of this research field to a large extent.[7] Excitedly, by utilizing the AIE concept, two efficient ML molecules, AIE-DF1

[a] *Department of Chemistry, Wuhan University, Wuhan 430072, China. E-mail: lizhen@whu.edu.cn, lichemlab@163.com*
[b] *PCFM Lab and GD HPPC Lab, State Key Laboratory of Optoelectronic Material and Technologies, School of Chemistry and Chemical Engineering, Sun Yat-sen University, Guangzhou 510275, China*

† Electronic supplementary information (ESI) available: Details of the synthesis; structure information of the compounds (NMR, IR, and mass spectra); Chart S1; Tables S1–S10; Fig. S1–S13. CCDC 1446198. For ESI and crystallographic data in CIF or other electronic format see DOI: 10.1039/c6mh00025h

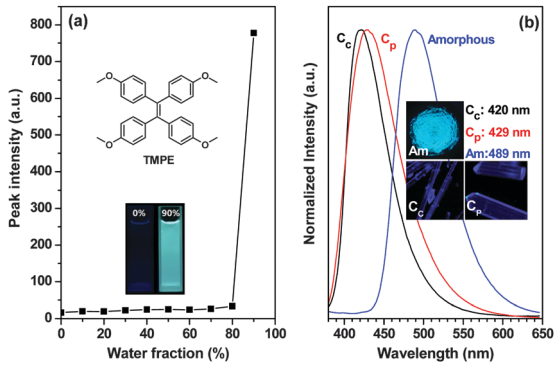

Fig. 1 (a) Change in PL peak intensity in a dilute solution of TMPE in water/THF mixtures with different water fractions (f_w). The inset depicts the emission images of TMPE in pure THF (left) and in 90% water fraction mixtures (right) under 365 nm UV illumination (10 μM). (b) PL spectra of TMPE in different phases. The inset depicts the emission images of TMPE in different phases; from left to right: crystal C_c-form, crystal C_p-form and amorphous sample (top) upon excitation at 365 nm.

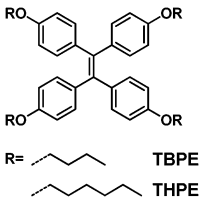

Chart 1 Molecular structures of TBPE and THPE.

and P4TA with relatively high polarity, were reported by Chi *et al.* in 2015 (Chart S1, ESI†).[8] However, it is a pity that both molecules are not stable enough in the presence of oxidant, even during storage in air. Furthermore, in addition to the few efficient ML materials reported so far, there were few powerful proofs giving a clear clue about the influence of the molecule packing pattern in the crystalline state on the ML properties. The lack of understanding regarding the mechanoluminescence–structure relationship has resulted in the bottleneck for the further development of this research field.

Intrigued by the previous excellent examples, and with the aim of exploring stable, nonpolar ML materials with efficient emission in the solid state, in this communication a polymorphic system constructed using 1,1,2,2-tetrakis(4-methoxyphenyl)ethane (TMPE) is presented (Fig. 1a), which is nonpolar, very stable against oxidation in air, and has AIE characteristics. By elaborately adjusting the solvent mixture, two crystalline polymorphs of TMPE were obtained with different space groups of $P2_1(c)$ (CCDC 921515) and $C2$ (CCDC 921516).[10c] Interestingly, the $P2_1(c)$ crystal (named as C_p-form), demonstrates wonderful ML properties, while the $C2$ crystal (named as C_c-form) is ML inactive, giving the possibility of investigating the solid-state structural requirements for ML activity from the same molecule and the same excited state.

By analysing the crystal structures of TMPE and its analogues carefully (Chart 1), it is concluded that the special molecular packing of TMPE accounts for its exciting efficient ML performance, which locks the non-radiative channels largely by almost restricting possible intermolecular motion, much similar to the inherent mechanism of RIM for AIE phenomena, thus providing a new insight for the development of efficient ML materials through crystal engineering besides molecular design.

The UV-visible absorption spectrum of TMPE was measured in a tetrahydrofuran (THF) solution. As shown in Fig. S1a (ESI†), there are two absorption bands centered at 259 and 329 nm, which are attributed to the π–π* local electron transition of the conjugated system. As it is constructed from the TPE (tetraphenylethene) unit, TMPE displays distinct AIE features. The compound is not emissive in good solvents like THF and DCM. However, when water, a poor solvent for TMPE, is added into its THF solution, the well-dissolved molecules would aggregate and induce the enhancement of emission. The aggregation is verified by the bathochromic shift and enhancement of the two absorption bands in the water/THF mixture (f_w = 90%). As shown in Fig. 1a, when the water fraction (f_w) is lower than 80%, the solution of TMPE has nearly no emission because of the free rotation of the carbon–carbon single bonds between the four periphery phenyls and the ethylene core. However, when f_w is higher than 80%, the emission peak centered at 492 nm appeared and was enhanced greatly when f_w was 90%.

Two different crystals of TMPE were cultured by slow solvent evaporation at room temperature. Accordingly, block-like crystals (C_p-form) were obtained from a solvent mixture of methanol and DCM, while another type of prism-like crystals (C_c-form) were obtained from the solvent mixture of *n*-hexane and DCM. The morphology images of these two different crystals are shown in Fig. 2a, and could be easily distinguished by the naked eye. The C_c-form crystal had a much bigger aspect ratio (~20) than the C_p-form (~1.5). It must be noted that there are two types of morphology for the C_c-form, one is a thin prism-like crystal (type A) and another consists of a bunch of prism-like ones (type B). The ML experiment for the C_c-form was performed on the type B crystals because type A were too tiny to apply force on them (and also as type A is ML inactive), and the larger size of the crystal provided a stronger PL emission upon grinding if it is ML active and could be observed more easily.[9]

Both of the two types of crystal emitted intense deep-blue fluorescence under UV illumination at room temperature (Fig. 4b and c). As shown in Table S1 (ESI†), the maximum emission wavelength of the C_c-form crystal (420 nm, $\Phi_{F,S}$ = 67.4%) exhibited a blue-shift compared to that of the C_p-form crystal

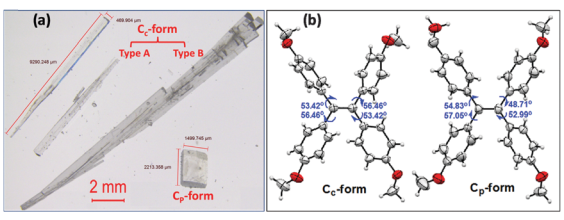

Fig. 2 (a) The polycrystalline morphology image of the C_c-form and C_p-form taken using an optic microscope Leica M123. (b) ORTEP drawings (50% probability ellipsoids) and selected dihedral angles (deg) in the C_c-form and C_p-form crystals.

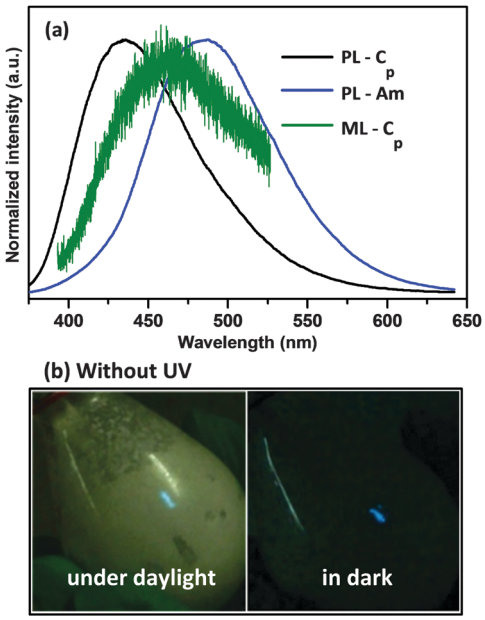

Fig. 3 (a) PL and ML spectra of TMPE in different phases: (PL-C_p) PL spectrum of the C_p-form crystal upon excitation at 331 nm; (PL-Am) PL spectrum of the amorphous compound upon excitation at 331 nm; (ML-C_p) ML spectrum of the C_p-form crystal upon grinding without UV illumination. (b) ML images of the as-prepared TMPE sample upon grinding with a spatula under daylight (left) and in the dark (right) at room temperature.

(429 nm, $\Phi_{F,s}$ = 69.9%). Analysis of the intermolecular interactions from the crystal packing data demonstrates that no π–π interactions or any type of H or J-aggregation exist in either crystal due to their propeller shape (Fig. S5 and S7, ESI†). The nearest distance between two aromatic planes of neighbouring TMPE molecules is larger than 4.2 Å. Therefore, the differences in the emission features should be derived from their different conformations, which are affected by the packing modes in the crystals. This idea was confirmed by the differences in the average value of the torsion angles of the phenyl rings between these two crystal types.[10a,11] For the C_c-form, the value was 54.94°, while it was 53.39° for the C_p-form. The smaller average value of the torsion angle of the phenyl rings induces better conjugation of the molecule. It perfectly explained the morphology dependent emissions of such propeller-shaped molecules: the C_c-form crystal exhibited a slightly blue-shifted (9 nm) emission rather than the C_p-form one. Also, compared to the crystal phase, the amorphous sample ($\Phi_{F,s}$ = 67.0%) displayed a large red-shifted (60 nm) emission centered at 489 nm. As we explained before, this was caused by the better conjugation of molecules when the crystal packing pattern was broken up.[10b]

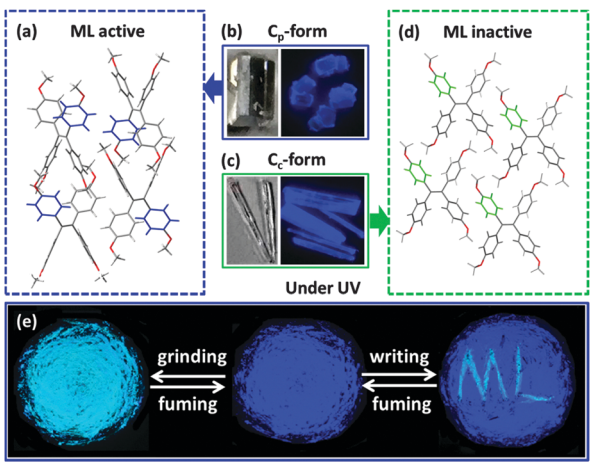

Fig. 4 (a) Stacking mode of the ML-active C_p-form crystal. (b) Images of the C_p-form crystal under daylight (left) and under an excitation of 365 nm UV light (right). (c) Images of the C_c-form crystal under daylight (left) and under an excitation of 365 nm UV light (right). (d) Stacking mode of the ML-inactive C_c-form crystal. (e) Images of reversible mechanochromic fluorescence under grinding/fuming and writable mechanochromic fluorescence of TMPE demonstrated by the capital letters 'ML' generated with an agate rod.

By grinding the C_p-form crystals with a pestle or shearing them with a spatula, a deep-blue light emission centered at 460 nm was observed in the dark or under daylight without UV irradiation (Fig. 3). The emission peak of the ML spectrum is located between the peaks of the PL spectra of the C_p-form crystal (429 nm) and amorphous compound (489 nm). It is worth mentioning that not only the C_p-form crystals had ML properties, but the as-prepared microcrystalline powder also emitted an apparent deep-blue light upon grinding with a spatula (Fig. 3b). On the contrary, the C_c-form crystal was ML inactive. So, what is the mechanoluminescence–structure relationship in the polymorphs of TMPE? More detailed investigation and analysis should be undertaken based on the single crystal data and other experimental results.

Generally, the intensity of the PL emission could remarkably increase at low temperatures. Thus, the influence of the temperature on the ML behaviour was investigated carefully. After the as-prepared microcrystal solid of TMPE in a flask was treated at different temperatures (77 K, 195 K, 233 K, 284 K, 323 K, 373 K) for 5 minutes, the sample was pulled out and immediately ground outside. As shown in the images (Fig. S4, ESI†), it was easily seen that the ML intensity increased with decreasing temperature, indicating that the non-radiative deactivation process was effectively suppressed at low temperature.

The powder X-ray diffraction (PXRD) spectra obviously exhibited different patterns for the two crystal samples (Fig. S2, ESI†). The C_p-form crystal had much better compressive resistance than the C_c-form. Under a light grinding force, the micro crystal powder of the C_p-form still exhibited sharp and high diffraction peaks. On the contrary, the micro crystal powder of the C_c-form demonstrated similar patterns to the amorphous with a similar grinding force, indicating that the well-ordered crystalline phase was thoroughly destroyed by grinding. Accordingly, the C_p-form crystal was also converted to an amorphous powder when ground thoroughly.

Although the two different crystal forms display distinct performances in ML activity, they show similar mechanofluorochromic performances, which are caused by the phase transition from crystalline to amorphous. The fluorescence of TMPE crystals can change from deep blue to cyan by grinding, and almost go back to the original deep blue emission again

immediately upon fuming treatment with good solvents like dichloromethane. Thus, it could demonstrate a good performance with high sensitivity and low background noise when writing the capital letters "ML" with an agate rod on the fumed samples, and erase them upon fuming with dichloromethane (Fig. 4e). These results have been reported and discussed carefully by Dong and Zhang in previous works.[10a,c,d] And usually, piezofluorochromic properties are associated with the piezoelectric effect, which is considered to be a possible process for ML.[7c,11]

To explore the underlying reason for the mechanoluminescence in the polymorphs of TMPE, structure analysis of these two single crystals was further performed to establish the structure–property relationship. Table S1 (ESI†) shows the basic single crystal information and ML activities of TMPE in different polymorphs. Both of them belong to the monoclinic crystal system. The space group of the C_c-form is $C2$, and $P2_1(c)$ for the C_p-form. The C_p-form crystal is non-centrosymmetric and the C_c-form crystal is centrosymmetric, which is associated with their different stacking patterns. The most notable difference between the two polymorphs is the θ between the ethylenic bonds of adjacent molecules, which represents the packing mode of the crystal (Fig. S9, ESI†). The conformation of TMPE was parallel (θ = 0°) in the C_c-form, while in contrast the conformation of TMPE was vertical (θ = 89.319°) in the C_p-form, showing that adjacent molecules were packed in a vertical arrangement. This difference in packing mode results in totally different C–H···π and C–H···O interactions in the polymorphs crystals (Table 1). There are 4 kinds of intermolecular C–H···π interactions (with distances ranging from 2.805 Å to 3.362 Å) and 3 kinds of intramolecular (with distances ranging from 3.288 Å to 3.539 Å) in the C_c-form crystal (Fig. S6 and Table S2, ESI†). In comparison with the C_c-form crystal, the C_p-form has many more intermolecular C–H···π interactions (Fig. S8 and Table S4, ESI†), which means more intense intermolecular forces between molecules. There are as many as 15 kinds of intermolecular C–H···π interactions (with distances ranging from 2.626 Å to 3.837 Å). Besides this, there are another 8 kinds of intramolecular C–H···π interactions in the C_p-form crystal (with distances ranging from 3.307 Å to 3.667 Å). Also, in addition to the different kinds of C–H···π interactions, there are different numbers of C–H···π interactions for each kind in one molecule. There are 6 intramolecular C–H···π hydrogen bonds (3 different kinds) between the four benzene rings in a single molecule of the C_c-form crystal, while 8 intramolecular C–H···π hydrogen bonds (8 different kinds) exist in the C_p-form crystal. Besides the small difference in the intramolecular C–H···π hydrogen bonds, more importantly, the difference in the intermolecular C–H···π hydrogen bonds is much larger both in quantity and intensity. The quantity of the C–H···π hydrogen bonds is almost 4-fold in the C_p-form crystal than that in the C_c-form. Due to the existence of oxygen atoms in the molecule, another kind of C–H···O intermolecular bond could not be ignored. It is not surprising to find that there are also remarkable differences between the two kinds of crystals here. There are in total 13 kinds of C–H···O intermolecular hydrogen bonds (with distances ranging from 2.833 Å to 3.964 Å) in the C_c-form crystal but as many as 24 kinds of C–H···O intermolecular hydrogen bonds (with distances ranging from 2.695 Å to 3.916 Å) in the C_p-form crystal (Tables S3 and S5, respectively, ESI†). The quantity of C–H···O intermolecular hydrogen bonds is almost 2-fold in the C_p-form crystal that of the C_c-form. As presented in the brackets above, the lengths of the intermolecular C–H···O hydrogen bonds and C–H···π interactions are shorter in the C_p-form crystal, rather than in the C_c-form, indicating stronger interactions in the former crystal. Based on these data, we could draw the conclusion that the greater number and stronger interactions in the C_p-form crystal make it pack in a more rigid molecular conformation and impedes intramolecular rotation, which largely reduces the energy loss *via* non-radiative relaxation channels under the stimulus of a force. Actually, another example could confirm this deduction from another side. During the preparation of TMPE, some analogues, TBPE and THPE (Chart 1),[12] were also synthesized/considered for comparison, with longer alkyl chains rather than the methyl one in TMPE. From their crystals (Fig. S10 and S11, ESI†), just like the C_c-form crystal of TMPE, there are fewer and weaker intermolecular C–H···O hydrogen bonds and C–H···π interactions, which is consistent with their inactive ML properties.

As mentioned above, the introduction of the TPE unit contributes to its unique AIE features, ensuring its strong emission in the solid state and providing the possibility of being an ideal pure organic ML material with bright light. The restriction of intramolecular motion (RIM) in the aggregates was identified as the main cause for the AIE effect. According to fundamental physics, it is believed that any movement, micro- or macroscopic alike, consumes energy. The intramolecular motion of aromatic rotors in AIE gens are active in the solution state, serving as a relaxation channel for its excitons to non-radiative decay. However, in the solid state, the intramolecular motions are restricted due to the physical constraint, which blocks the non-radiative pathway and opens a radiative channel. Thus, the restriction of intramolecular motion leads to enhanced emission in the solid state.[2i,j] Based on what we have been discussed above, we can draw lessons from the AIE mechanism to explain why the different crystal forms of TMPE display contrasting ML activity. As discussed above, the neighbouring molecules in the C_c-form crystal are parallel, while on the contrary they are vertical in the C_p-form crystal. This vertical conformation leads to more compact stacking and more intermolecular interactions in the crystal. Moreover, the crossed conformation makes the molecules in the crystal lock to each other to improve the

Table 1 Summary of the C–H···π and C–H···O interactions in the different polymorph crystals

Crystal form	Intramolecular C–H···π		Intermolecular C–H···π		C–H···O	
C_c-form	3[a]	6[b]	4	8	13	26
	3.288–3.539[c] Å		2.805–3.362 Å		2.833–3.964 Å	
C_p-form	8	8	15	30	24	48
	3.307–3.667 Å		2.626–3.837 Å		2.695–3.916 Å	

[a] The number of kinds of hydrogen bonds. [b] The number of hydrogen bonds. [c] The distance range of hydrogen bonds.

rigidity of the crystal. The PXRD data of the crystals before and after grinding under the same strength of force confirmed that the C_p-form crystal is much more rigid than the C_c-form. Additional details observed in the grinding process also support this point. Upon grinding with a spatula, the block-like crystals (C_p-form) were broken into smaller block-like ones accompanied by a blue light, and the light will not die out until the smaller crystals were thoroughly changed into an amorphous powder. On the contrary, under the same conditions, the bunched prism-like crystals (C_c-form) were easily turned into amorphous powder without any emission. Some previous reports have suggested that the fracture of crystals and the concomitant creation of new surfaces in the crystal are responsible for ML excitation, which is consistent with the results we obtained.[11] When force is placed on crystals by grinding them with spatula, the C_c-form crystal collapses and changes into an amorphous powder, and mechanical energy is released in a non-radiative pathway by the slippage of molecules, resulting in disruption of the crystal. However, for the C_p-form crystal, the more rigid molecular stacking mode and stronger interactions between molecules block the non-radiative pathway by decreasing molecular slippage, and the large crystals fracture and change into smaller crystals accompanied by an easily observed blue light as the radiative channel is opened. The fracture process would continue and the blue light remains until the micro-crystal structure decomposes completely.

Classical B3LYP density functional theory was also used to calculate the conformations at the 6-31G(d,p) level based on their ground state geometries in the single crystals. As shown in Fig. S12 (ESI†), there is no distinct orbital delocalization because there is no D–A structure in TMPE. The C_p-form crystal has a smaller ΔE_g (HOMO–LUMO) value at 4.23 eV compared to the C_c-form (4.29 eV). These calculations are in good agreement with the solid state UV-visible spectra of the C_g-form and C_c-form crystals which absorbed at 380 nm and 372 nm, respectively (Fig. S1b, ESI†). These results indicate that the electrons of molecules in the C_p-form can be excited with a lower energy compared to the C_c-form.[8b]

In summary, by carefully utilizing different solvents, two crystalline polymorphs (C_p-form and C_c-form) were successfully obtained for the nonpolar, stable TMPE molecule with AIE characteristics. Regardless of the same molecular structure, the two crystals show opposite mechanoluminescence activities, derived from their different conformations of packing modes in the crystals. While the C_c-form is ML inactive, the block-like C_p-form exhibits blue emission upon grinding due to the greater and stronger intermolecular C–H$\cdots$O hydrogen bonds and C–H$\cdots\pi$ interactions, which largely reduce the possible energy loss *via* non-radiative relaxation channels by decreasing the molecular slippage under the stimulus of force. The outstanding ML performance of TMPE, coupled with its AIE characteristics and high stability in air, give it potential applications in display and sensor fields. More importantly, the clear relationship between the packing in the crystal and the ML properties can provide some guidance for the design of efficient organic ML materials.

Acknowledgements

We are grateful to the National Fundamental Key Research Program (2013CB834701), and the National Science Foundation of China (no. 21325416, 51573140) for financial support.

References

1 (*a*) S. W. Thomas, G. D. Joly and T. M. Swager, *Chem. Rev.*, 2007, **107**, 1339–1386; (*b*) R. Yang, A. Garcia, D. Korystov, A. Mikhailovsky, G. C. Bazan and T.-Q. Nguyen, *J. Am. Chem. Soc.*, 2006, **128**, 16532–16539; (*c*) M. Levitus, G. Zepeda, H. Dang, C. Godinez, T.-A. V. Khuong, K. Schmieder and M. A. Garcia-Garibay, *J. Org. Chem.*, 2001, **66**, 3188–3195.

2 (*a*) J. Luo, Z. Xie, J. W. Y. Lam, L. Cheng, B. Z. Tang, H. Chen, C. Qiu, H. S. Kwok, X. Zhan, Y. Liu and D. Zhu, *Chem. Commun.*, 2001, 1740–1741; (*b*) J. Chen, C. C. W. Law, J. W. Y. Lam, Y. Dong, S. M. F. Lo, I. D. Williams, D. Zhu and B. Z. Tang, *Chem. Mater.*, 2003, **15**, 1535–1546; (*c*) G. Yu, S. Yin, Y. Liu, J. Chen, X. Xu, X. Sun, D. Ma, X. Zhan, Q. Peng, Z. Shuai, B. Z. Tang, D. Zhu, W. Fang and Y. Luo, *J. Am. Chem. Soc.*, 2005, **127**, 6335–6346; (*d*) X. Fan, J. Sun, F. Wang, Z. Chu, P. Wang, Y. Dong, R. Hu, B. Z. Tang and D. Zou, *Chem. Commun.*, 2008, 2989–2991; (*e*) Z. Li, Y. Dong, B. Mi, Y. Tang, M. Haeussler, H. Tong, Y. Dong, J. W. Y. Lam, Y. Ren, H. H. Y. Sung, K. S. Kwok and B. Z. Tang, *J. Phys. Chem. B*, 2005, **109**, 10061–10066; (*f*) H. Wang, E. G. Zhao, J. W. Y. Lam and B. Z. Tang, *Mater. Today*, 2015, **18**, 365–377; (*g*) J. Mei, N. L. C. Leung, R. T. K. Kwok, J. W. Y. Lam and B. Z. Tang, *Chem. Rev.*, 2015, **115**, 11718–11940; (*h*) R. T. K. Kwok, C. W. T. Leung, J. W. Y. Lam and B. Z. Tang, *Chem. Soc. Rev.*, 2015, **44**, 4228–4238; (*i*) R. Hu, N. L. C. Leung and B. Z. Tang, *Chem. Soc. Rev.*, 2014, **43**, 4494–4562; (*j*) Y. N. Hong, J. W. Y. Lam and B. Z. Tang, *Chem. Commun.*, 2009, 4332–4353.

3 (*a*) N. L. C. Leung, N. Xie, W. Z. Yuan, Y. Liu, Q. Y. Wu, Q. Peng, Q. Miao, J. W. Y. Lam and B. Z. Tang, *Chem. – Eur. J.*, 2014, **20**, 15349–15353; (*b*) T. Virgili, A. Forni, E. Cariati, D. Pasini and C. Botta, *J. Phys. Chem. C*, 2013, **117**, 27161–27166; (*c*) J. Liu, H. Su, L. Meng, Y. Zhao, C. Deng, J. C. Y. Ng, P. Lu, M. Faisal, J. W. Y. Lam, X. Huang, H. Wu, K. S. Wong and B. Z. Tang, *Chem. Sci.*, 2012, **3**, 2737–2747; (*d*) C. Deng, Y. Niu, Q. Peng, A. Qin, Z. Shuai and B. Z. Tang, *J. Chem. Phys.*, 2011, **135**, 014304; (*e*) E. P. J. Parrott, N. Y. Tan, R. Hu, J. A. Zeitler, B. Z. Tang and E. Pickwell-MacPherson, *Mater. Horiz.*, 2014, **1**, 251–258.

4 (*a*) J. Huang, N. Sun, Y. Dong, R. Tang, P. Lu, P. Cai, Q. Li, D. Ma, J. Qin and Z. Li, *Adv. Funct. Mater.*, 2013, **23**, 2329–2337; (*b*) J. Huang, N. Sun, J. Yang, R. Tang, Q. Li, D. Ma and Z. Li, *Adv. Funct. Mater.*, 2014, **24**, 7645–7654; (*c*) X. Xu, J. Huang, J. J. Li, J. Yan, J. Qin and Z. Li, *Chem. Commun.*, 2011, **47**, 12385–12387; (*d*) W. Wu, S. Ye, L. Huang, L. Xiao, Y. Fu, Q. Huang, G. Yu, Y. Liu, J. Qin, Q. Li and Z. Li, *J. Mater. Chem.*, 2012, **22**, 6374–6382; (*e*) C. W. T. Leung, Y. Hong, S. Chen, E. Zhao, J. W. Y. Lam and B. Z. Tang, *J. Am. Chem. Soc.*, 2013, **135**, 62–65;

(*f*) Y. Yuan, C.-J. Zhang, M. Gao, R. Zhang, B. Z. Tang and B. Liu, *Angew. Chem., Int. Ed.*, 2015, **54**, 1780–1786; (*g*) Z. Xie, C. Chen, S. Xu, J. Li, Y. Zhang, S. Liu, J. Xu and Z. Chi, *Angew. Chem., Int. Ed.*, 2015, **54**, 7181–7184; (*h*) P. Duan, N. Yanai, Y. Kurashige and N. Kimizuka, *Angew. Chem., Int. Ed.*, 2015, **54**, 7544–7549; (*i*) J. Zhao, D. Yang, Y. Zhao, X.-J. Yang, Y.-Y. Wang and B. Wu, *Angew. Chem., Int. Ed.*, 2014, **53**, 6632–6636; (*j*) J. Li, Y. Li, C. Y. K. Chan, R. T. K. Kwok, H. Li, P. Zrazhevskiy, X. Gao, J. Z. Sun, A. Qin and B. Z. Tang, *Angew. Chem., Int. Ed.*, 2014, **53**, 13518–13522; (*k*) Q. Hu, M. Gao, G. Feng and B. Liu, *Angew. Chem., Int. Ed.*, 2014, **53**, 14225–14229; (*l*) D. Yan and D. G. Evans, *Mater. Horiz.*, 2014, **1**, 46–57; (*m*) X. Ji, P. Wang, H. Wang and F. Huang, *Chin. J. Polym. Sci.*, 2015, **33**, 890–898; (*n*) H. Li, J. Cheng, Y. Zhao, J. W. Y. Lam, K. S. Wong, H. Wu, B. S. Li and B. Z. Tang, *Mater. Horiz.*, 2014, **1**, 518–521; (*o*) D. Ding, R. T. K. Kwok, Y. Y. Yuan, G. X. Feng, B. Z. Tang and B. Liu, *Mater. Horiz.*, 2015, **2**, 100–105.

5 (*a*) N. C. Eddingsaas and K. S. Suslick, *Nature*, 2006, **444**, 163; (*b*) N. C. Eddingsaas and K. S. Suslick, *J. Am. Chem. Soc.*, 2007, **129**, 6718–6719; (*c*) J. I. Zink and W. C. Kaska, *J. Am. Chem. Soc.*, 1973, **95**, 7510–7512; (*d*) J. I. Zink and W. Klimt, *J. Am. Chem. Soc.*, 1974, **96**, 4690–4692.

6 J. Picard, *Science*, 1939, **89**, 460.

7 (*a*) J. I. Zink, G. E. Hardy and J. E. Sutton, *J. Phys. Chem.*, 1976, **80**, 248–249; (*b*) J. I. Zink, *Acc. Chem. Res.*, 1978, **11**, 289–295; (*c*) G. E. Hardy, W. C. Kaska, B. P. Chandra and J. I. Zink, *J. Am. Chem. Soc.*, 1981, **103**, 1074–1079; (*d*) H. Nakayama, J.-i. Nishida, N. Takada, H. Sato and Y. Yamashita, *Chem. Mater.*, 2012, **24**, 671–676; (*e*) J. Nishida, H. Ohura, Y. Kita, H. Hasegawa, T. Kawase, N. Takada, H. Sato, Y. Sei and Y. Yamashita, *J. Org. Chem.*, 2016, **81**, 433–441.

8 (*a*) S. D. Xu, T. Liu, Y. Mu, Y. Wang, Z. Chi, C. C. Lo, S. Liu, Y. Zhang, A. Lien and J. Xu, *Angew. Chem., Int. Ed.*, 2015, **54**, 874–878; (*b*) B. J. Xu, J. J. He, Y. X. Mu, Q. Z. Zhu, S. K. Wu, Y. F. Wang, Y. Zhang, C. J. Jin, C. C. Lo, Z. G. Chi, A. Lien, S. W. Liu and J. R. Xu, *Chem. Sci.*, 2015, **6**, 3236–3241.

9 P. Jha and B. P. Chandra, *Luminescence*, 2014, **29**, 977–993.

10 (*a*) C. Li, X. Luo, W. Zhao, C. Li, Z. Liu, Z. Bo, Y. Dong, Y. Q. Dong and B. Z. Tang, *New J. Chem.*, 2013, **37**, 1696–1699; (*b*) Y. Q. Dong, J. W. Lam and B. Z. Tang, *J. Phys. Chem. Lett.*, 2015, **6**, 3429–3436; (*c*) Q. Qi, Y. Liu, X. Fang, Y. Zhang, P. Chen, Y. Wang, B. Yang, B. Xu, W. Tian and S. X.-A. Zhang, *RSC Adv.*, 2013, **3**, 7996–8002; (*d*) J. Wu, J. Tang, H. Wang, Q. Qi, X. Fang, Y. Liu, S. Xu, S. X. Zhang, H. Zhang and W. Xu, *J. Phys. Chem. A*, 2015, **119**, 9218–9224.

11 (*a*) B. P. Chandra and J. I. Zink, *Inorg. Chem.*, 1980, **19**, 3098–3102; (*b*) J. I. Zink, *Naturwissenschaften*, 1981, **68**, 507–512; (*c*) B. P. Chandra and J. I. Zink, *Phys. Rev. B: Condens. Matter Mater. Phys.*, 1980, **21**, 816–826.

12 X. Luo, W. Zhao, J. Shi, C. Li, Z. Liu, Z. Bo, Y. Q. Dong and B. Z. Tang, *J. Phys. Chem. C*, 2012, **116**, 21967–21972.